Entangling the whole by beam splitting a part

Callum Croal*,[1] Christian Peuntinger*,[2, 3] Vanessa Chille,[2, 3] Christoph
Marquardt,[2, 3] Gerd Leuchs,[2, 3] Natalia Korolkova,[1] and Ladislav Mišta, Jr.[4]

[1]*School of Physics and Astronomy, University of St. Andrews,
North Haugh, St. Andrews, Fife, KY16 9SS, Scotland*
[2]*Max Planck Institute for the Science of Light, Günther-Scharowsky-Str. 1/Bldg. 24, Erlangen, Germany*
[3]*Institute of Optics, Information and Photonics,
University of Erlangen-Nuremberg, Staudtstraße 7/B2, Erlangen, Germany*
[4]*Department of Optics, Palacký University, 17. listopadu 12, 771 46 Olomouc, Czech Republic*
(Dated: July 6, 2015)

A beam splitter is a basic linear optical element appearing in many optics experiments and is frequently used as a continuous-variable entangler transforming a pair of input modes from a separable Gaussian state into an entangled state. However, a beam splitter is a passive operation that can create entanglement from Gaussian states only under certain conditions. One such condition is that the input light is suitably squeezed. We demonstrate experimentally that a beam splitter can create entanglement even from modes which do not possess such a squeezing provided that they are correlated to but not entangled with a third mode. Specifically, we show that a beam splitter can create three-mode entanglement by acting on two modes of a three-mode fully separable Gaussian state without entangling the two modes themselves. This beam splitter property is a key mechanism behind the performance of the protocol for entanglement distribution by separable states. Moreover, the property also finds application in collaborative quantum dense coding in which decoding of transmitted information is assisted by interference with a mode of the collaborating party.

A beam splitter (BS) is an optical device that can superimpose incident light modes. As quadrature amplitudes of the incoming modes are also superimposed in this process, correlations may arise between the corresponding quadratures of the output modes. In particular, if modes squeezed in conjugate quadratures enter a BS, an entangled state carrying Einstein-Podolsky-Rosen correlations [1] emerges at the output [2, 3]. This is currently a widely used experimental method, which finds application in continuous-variable (CV) quantum teleportation [2], dense coding [4] or cryptography [5, 6].

Whether entanglement will be created by a BS depends on the nature of the input states. For classical input states given by statistical mixtures of coherent states the output states are also classical [7] and thus possess no entanglement. Therefore, to get entanglement on a BS some non-classicality is needed at the input [8, 9]. In CV experiments non-classicality of Gaussian states [10] is used for this purpose which is equivalent to squeezing [11]. However, the mere presence of some input squeezing may not suffice for the generation of entanglement on a BS [8]. It requires more stringent conditions [12]. An interesting question that arises is whether interference on a BS of some states which do not satisfy the condition and hence do not entangle on a BS can still create some entanglement. Remarkably, this is indeed possible if the interfered state is a local state of a fully separable state of a larger system. This is illustrated by the protocol for Gaussian entanglement distribution by separable states [13] where a BS creates entanglement by acting on two modes of a fully separable three-mode Gaussian state while leaving the modes individually disentangled. Note, that so far such a property of a BS has not been demonstrated, because in the experiment [14] the addi-

tional third mode was independent of the superimposed modes, whereas in the experiment [15], the third mode was entangled with one of the modes entering the BS.

In this Letter we provide an experimental demonstration of the property of a BS mentioned above using two examples. In the first example the initial separable state is two-mode and it is prepared by random displacements of a squeezed state and a vacuum state in one quadrature. By splitting the former state on a BS we then create a three-mode state in which the output modes of the BS are separable individually but simultaneously each output mode is entangled with the remaining two modes. In the second example we prepare a three-mode fully separable state by random displacement of two orthogonally squeezed states in the squeezed quadratures and the vacuum state in both quadratures. By superimposing originally squeezed states on a BS we then create an entangled state in which the output modes of the BS are again separable but one of the output modes is entangled with the remaining two modes at the same time. The state from the first (second) example is a backbone of the CV protocol for entanglement sharing [16] (distribution [13]) with separable states. Moreover, despite being partially separable and noisy, the states also enable assisted quantum dense coding which can beat coherent-state and even squeezed-state communication capacity.

We demonstrate the aforementioned effect using quantum modes of the electromagnetic field, which are quantum systems with infinite-dimensional Hilbert spaces. A system of n modes is described by the vector of quadratures $\hat{\boldsymbol{\xi}} = (\hat{x}_1, \hat{p}_1, ..., \hat{x}_n, \hat{p}_n)$, the elements of which satisfy the canonical commutation rules $[\hat{\xi}_j, \hat{\xi}_k] = i(\boldsymbol{\Omega}_n)_{jk}$, with $\boldsymbol{\Omega}_n = \oplus_{j=1}^n i\boldsymbol{\sigma}_y$, where $\boldsymbol{\sigma}_y$ is the Pauli-y matrix. Quantum states involved in our experiment are well ap-
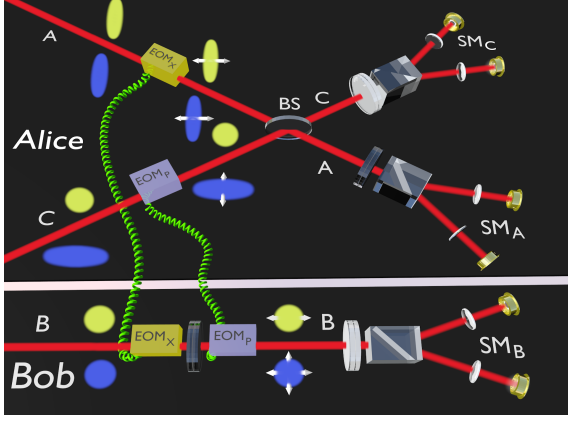
FIG. 1: Experimental scheme. EOM_i: electro-optical modulator displacing quadrature i, BS: balanced beam splitter, SM_j: Stokes measurement on mode j. The yellow (blue) circles and ellipses represent the states of protocol 1 (2). The yellow modulators EOM_x are applied to both protocols and the blue modulators EOM_p are only applied to protocol 2.

proximated by Gaussian states [14], i.e., states with a Gaussian Wigner function, and we resort to the tools of Gaussian quantum information theory [10] in what follows.

A Gaussian state $\hat{\rho}$ is fully characterized by the vector of first moments $\langle \hat{\boldsymbol{\xi}} \rangle \equiv \mathrm{Tr}(\hat{\boldsymbol{\xi}}\hat{\rho})$, which is always zero in the present case, and the covariance matrix (CM) $\boldsymbol{\gamma}$ with elements $\gamma_{jk} = \langle \hat{\xi}_j\hat{\xi}_k + \hat{\xi}_k\hat{\xi}_j \rangle - 2\langle \hat{\xi}_j \rangle \langle \hat{\xi}_k \rangle$. An important property of a Gaussian state is its non-classicality. We say that a state is non-classical if it cannot be expressed as a statistical mixture of coherent states [17, 18]. In the Gaussian scenario, non-classicality is equivalent with squeezing [11], i.e., a Gaussian state with CM $\boldsymbol{\gamma}$ is non-classical if and only if (iff) $\mu := \min[\mathrm{eig}(\boldsymbol{\gamma})] < 1$ [19].

In the present experiment we generate three-mode states with specific separability properties. We certify the properties using the positive partial transpose (PPT) criterion for Gaussian states [20–22]. The partial transposition operation with respect to mode j transforms an n-mode CM $\boldsymbol{\gamma}$ to $\boldsymbol{\gamma}^{(T_j)} = \boldsymbol{\Lambda}_j\boldsymbol{\gamma}\boldsymbol{\Lambda}_j$ with $\boldsymbol{\Lambda}_j = (\oplus_{i \neq j=1}^{n} \mathbb{1}^{(i)}) \oplus \boldsymbol{\sigma}_z^{(j)}$, where $\mathbb{1}^{(i)}$ is the 2×2 identity matrix of mode i, and $\boldsymbol{\sigma}_z^{(j)}$ is the Pauli-z matrix of mode j. The PPT criterion then states that the state is separable with respect to mode j iff

$$\boldsymbol{\gamma}^{(T_j)} + i\boldsymbol{\Omega}_n \geq 0. \tag{1}$$

We demonstrate the entangling power of a BS on two protocols depicted in Fig. 1. First, we focus on a more simple protocol (yellow circles and ellipses in Fig. 1) which we shall refer to as protocol 1. Alice initially holds mode A in a position squeezed vacuum state with quadratures $\hat{x}_A = e^{-r}\hat{x}_A^{(0)}$, $\hat{p}_A = e^r\hat{p}_A^{(0)}$, where $r > 0$ is the squeezing parameter and the superscript "(0)" denotes the vacuum quadratures, while Bob holds a vac-

uum mode B with quadratures $\hat{x}_B = \hat{x}_B^{(0)}$ and $\hat{p}_B = \hat{p}_B^{(0)}$. Next, modes A and B are displaced as

$$\hat{x}_A \to \hat{x}_A + x, \quad \hat{x}_B \to \hat{x}_B + x, \tag{2}$$

where the classical displacement x is Gaussian distributed with zero mean and variance $\langle x^2 \rangle = V_1 := (1 - e^{-2r})/2$. The displacements realize an LOCC operation and the resulting state is thus separable. Further, the displacements are strong enough to destroy the initial squeezing and the state of mode A is classical. However, the lowest eigenvalue of the CM of the global state is equal to $\mu = e^{-r}[\cosh r - (\sqrt{5} - 2)\sinh r] < 1$ and hence the state is non-classical.

Mode A is then split on a BS realizing a transformation $\hat{x}_{A,C} \to (\hat{x}_A \pm \hat{x}_C)/\sqrt{2}$, $\hat{p}_{A,C} \to (\hat{p}_A \pm \hat{p}_C)/\sqrt{2}$, where $\hat{x}_C = \hat{x}_C^{(0)}$ and $\hat{p}_C = \hat{p}_C^{(0)}$ are quadratures of the vacuum mode C entering the empty port of the BS. Application of the BS results in a three-mode state with CM $\boldsymbol{\gamma}_1$, which carries no entanglement between any two modes and across the $B|AC$ splitting, but which is entangled across the $A|BC$ and $C|AB$ splittings [16]. The protocol 1 thus demonstrates the required entangling property of a BS. Indeed, we have created entanglement from a fully separable three-mode Gaussian state by mixing on a BS two modes of the state while these two modes alone remain separable after the BS.

The entangling capability of a BS can be also illustrated using a different protocol called protocol 2 in what follows (blue circles and ellipses in Fig. 1). Alice holds mode A in a position-squeezed state and mode C in a momentum squeezed state, and Bob holds mode B in a vacuum state. The modes are then displaced as

$$\begin{aligned} \hat{x}_A &\to \hat{x}_A + x, \quad \hat{x}_B \to \hat{x}_B + \sqrt{2}x, \\ \hat{p}_C &\to \hat{p}_C - p, \quad \hat{p}_B \to \hat{p}_B + \sqrt{2}p, \end{aligned} \tag{3}$$

where x and p are uncorrelated classical displacements obeying zero mean Gaussian distributions with variances $\langle x^2 \rangle = \langle p^2 \rangle = V_2 := (e^{2r} - 1)/2$. In comparison with protocol 1, the final state with CM $\boldsymbol{\gamma}_2$ of protocol 2 has different separability properties. Specifically, the state is separable across the $B|AC$ and $C|AB$ splittings, which guarantees absence of any two-mode entanglement, and it is entangled across the $A|BC$ splitting. Thus again, entanglement is created by mixing on a BS two modes of a three-mode fully separable Gaussian state, whereas the two modes at the output of the BS do not get entangled.

The experimental setup for both protocols is shown in Fig. 1. The implementation is realized using Stokes observables and measurements. A high excitation of $\hat{S}_3$ (circular polarization), and in contrast $\langle \hat{S}_1 \rangle = \langle \hat{S}_2 \rangle = 0$, allows the S_1-S_2-plane (also called "dark-plane"[23]) to be interpreted as the quadrature phase space. Within this plane $\hat{S}_\theta$ ($\hat{S}_{\theta+\pi/2}$) is identified with the $\hat{x}$ ($\hat{p}$) quadrature. In both scenarios Alice possesses two modes A and C and Bob holds mode B. All the involved modes (except mode C in the first protocol, which is a real vacuum

mode) are created with a soliton laser (Origami, One-five, center wavelength: 1559 nm, pulse length: 200 fs, repetition rate: 80 MHz). Mode A initially exhibits polarization squeezing in $\hat{S}_\theta$ ($\hat{x}$), generated by using the Kerr nonlinearity of an optical fiber (FS-PM-7811, Thorlabs, 13 m) [3, 23–25]. This initial squeezing is destroyed by modulation in the squeezing direction $\hat{S}_\theta$ realized in two steps. First, different displacements are realized by slightly modulating the state of polarization applying a sinusoidal voltage (frequency: 18.2 MHz) to an electro optical modulator (EOM) and electronically down-mixing the Stokes measurement signal with a phase matched local oscillator of the same frequency. Second, digitally mixing measurements from different displaced modes leads to a mixed Gaussian state, which can be expressed as a statistical mixture of coherent states. In the simpler protocol this mode A is mixed with a vacuum mode C on a BS. Bob prepares mode B, initially coherent but modulated in the same manner and correlated to mode A of Alice. The CM $\boldsymbol{\gamma}_1$ was measured to be

$$\boldsymbol{\gamma}_1 = \begin{pmatrix} 5.42 & 0.23 & 3.34 & -0.73 & 4.06 & 0.04 \\ 0.23 & 19.28 & 0.00 & 0.00 & 0.45 & 17.29 \\ 3.34 & 0.00 & 3.43 & -0.54 & 3.06 & -0.03 \\ -0.73 & 0.00 & -0.54 & 1.12 & -0.67 & 0.01 \\ 4.06 & 0.45 & 3.06 & -0.67 & 4.73 & 0.55 \\ 0.04 & 17.29 & -0.03 & 0.01 & 0.55 & 17.70 \end{pmatrix}.$$

The measurement errors for the elements of all measured CMs lie between 0.002 and 0.023.

As for protocol 2, it uses the same mode A as the first one, but it is extended with a mode C. This mode C is prepared in the same way as mode A, just the squeezing and, accordingly, also the modulation are in the $\hat{S}_{\theta+\pi/2}$ direction. Again these two modes are mixed on a BS. In this case, Bob's mode B is independently modulated in both conjugate Stokes observables $\hat{S}_\theta$ and $\hat{S}_{\theta+\pi/2}$. In the case of protocol 2, the CM $\boldsymbol{\gamma}_2$ was measured to be

$$\boldsymbol{\gamma}_2 = \begin{pmatrix} 20.90 & 1.10 & 5.17 & -8.59 & -7.80 & -1.68 \\ 1.10 & 25.31 & -5.04 & -6.76 & 1.00 & 14.64 \\ 5.17 & -5.04 & 11.87 & -0.45 & 4.95 & 4.49 \\ -8.59 & -6.76 & -0.45 & 18.88 & -8.61 & 6.04 \\ -7.80 & 1.00 & 4.95 & -8.61 & 20.68 & 0.80 \\ -1.68 & 14.64 & 4.49 & 6.04 & 0.80 & 24.65 \end{pmatrix}.$$

The architecture of our experimental setup together with the separability properties of the measured CMs guarantee that we are able to really observe the predicted entangling capability of a BS. Note first, that the three-mode state before the BS has been prepared by local operations on independent modes and classical communication (green wires in Fig. 1) and therefore it is by construction fully separable. Further, by applying the separability criterion (1) on CMs $\boldsymbol{\gamma}_1$ and $\boldsymbol{\gamma}_2$ and the local CMs $\boldsymbol{\gamma}_{1,AC}$ and $\boldsymbol{\gamma}_{2,AC}$ of reduced states of modes A and C, we can confirm that the CMs also exhibit the desired separability properties.

The three-mode separability properties of the CMs $\boldsymbol{\gamma}_1$ and $\boldsymbol{\gamma}_2$ are summarized in Table I. For CM $\boldsymbol{\gamma}_1$, the two

TABLE I: Minimum eigenvalue $\lambda_k^{(T_j)} := \min[\mathrm{eig}(\boldsymbol{\gamma}_k^{(T_j)} + i\boldsymbol{\Omega}_3)]$.

j	A	B	C
$\lambda_1^{(T_j)} \times 10^2$	-2.2 ± 0.1	6.9 ± 0.1	-2.2 ± 0.1
$\lambda_2^{(T_j)} \times 10$	-1.44 ± 0.01	3.51 ± 0.02	5.28 ± 0.03

negative minimum eigenvalues in the table reveal that the BS created entanglement with respect to the $A|BC$ and $C|AB$ splittings, whereas the state is separable across the $B|AC$ splitting, as predicted by the theory. However, as required, at the same time modes A and C did not get entangled according to the criterion (1). This is evidenced by $\min[\mathrm{eig}(\boldsymbol{\gamma}_{1,AC}^{(T_A)} + i\boldsymbol{\Omega}_2)] = 0.84 \pm 0.01 > 0$.

Moving to the CM $\boldsymbol{\gamma}_2$, one can see from Table I that the CM represents an entangled state across the $A|BC$ splitting whereas it exhibits separability across the $B|AC$ and $C|AB$ splittings in accordance with the theory. Finally, since $\min[\mathrm{eig}(\boldsymbol{\gamma}_{2,AC}^{(T_A)} + i\boldsymbol{\Omega}_2)] = 9.371 \pm 0.005 > 0$ [14], modes A and C are separable as expected.

The present experiment demonstrates that a BS can create entanglement even by mixing two modes, which alone cannot be entangled by the BS. The condition under which this can happen is that the two modes are part of a three-mode fully separable system. The entanglement is created solely by the BS because no entanglement is present before the BS. The entanglement does not occur between the output modes of the BS but instead it emerges between one output mode and the remaining two modes taken together. This phenomenon is a key element of the protocols for entanglement sharing [16] and distribution [13, 26] with separable states. The schemes depicted in Fig. 1 are effectively the first two steps of these protocols. Thus a passive BS operation on a tailored three-mode fully separable state not only can generate entanglement across some bipartite splittings of a global state, but a further BS can localize this entanglement between modes A and B. This has been experimentally demonstrated for the entanglement sharing protocol in [27] and for the entanglement distribution protocol in [14]. In both cases, the recovery of two-mode entanglement has been performed electronically on the outcomes of the measurement on mode C and the presence of entanglement has been certified by the sufficient condition for entanglement [28].

Entanglement created in protocols 1 and 2 is not only useful for sharing and distribution of entanglement, but also directly finds an application in a collaborative version of quantum dense coding [29] with continuous variables [4, 30]. The corresponding scheme is depicted in Fig. 2. Comparing to the standard dense coding schemes containing only a sender Alice and a receiver Bob, in the collaborative schemes, Charlie controls the capacity of information transmission between Alice and Bob. While previous collaborative schemes [4, 31] were based on genuine tripartite entanglement and the control of capacity was accomplished by a measurement on Charlie's mode,
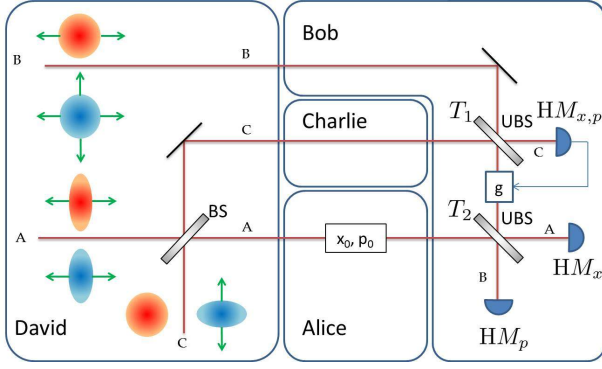
FIG. 2: Collaborative dense coding schemes with a state from protocol 1 (orange circles and ellipsis) and protocol 2 (blue circle and ellipses). BS: balanced beam splitter, UBS: unbalanced beam splitters with transmissivities T_1 and T_2, HM: homodyne measurement.

the present scheme relies only on a partially entangled tripartite state and it utilizes interference of the collaborator and receiver's mode for the control.

The schemes in Fig. 2 start with preparation of the output state of protocol 1 (2) about which the participants have no information. To emphasize this, we attribute the preparation to a separate party, David. After running protocol 1 (2) David distributes modes A, B and C of the state with CM γ_1 (γ_2) to Alice, Bob and Charlie. Alice encodes on her mode classical Gaussian signals x_0 and p_0 with variance P by performing displacements $\hat{x}_A \to \hat{x}_A + x_0$ and $\hat{p}_A \to \hat{p}_A + p_0$ and sends the mode to Bob. Upon receiving the mode, Bob decodes the signal with the help of Charlie in two steps depicted in Fig. 2. First, he superimposes his mode with mode C on an unbalanced BS $\hat{\alpha}'_{B,C} = R_1\hat{\alpha}_{C,B} \pm T_1\hat{\alpha}_{B,C}$, $\alpha = x, p$, measures the quadrature $\hat{p}'_C$ on output mode C with outcome $\bar{p}$, and displaces the other output mode B as $\hat{p}'_B \to \hat{p}'_B + g\bar{p}$, where a gain g maximizes the capacity. In the second step, Bob superimposes modes A and B on another unbalanced BS with transmissivity T_2 and measures the quadrature $\hat{x}$ ($\hat{p}$) on output mode A (B). Making use of the formula for capacity of a communication channel with Gaussian distributed signal (noise) of power S (N), $C = (1/2)\ln(1 + S/N)$ [32], we have then calculated the channel capacity (CC) C^j for the protocol j.

The CC has been optimized over the transmissivities T_1 and T_2 for fixed average photon number $\bar{n}$ and it is plotted in Fig. 3. For comparison, we plot also the capacities for coherent-state communication with heterodyne detection, $C^{\mathrm{coh}} = \ln(1 + \bar{n})$, and the squeezed-state communication with homodyne detection, $C^{\mathrm{sq}} = \ln(1 + 2\bar{n})$ [33]. Besides, we have also considered a third protocol 3 with the CC C^3, which is the same as protocol 2, but

with lower added noise $V_3 = V_1$, causing the entanglement properties of the output state to be the same as in protocol 1.

In all schemes, if mode B or C is ignored, the CC never exceeds C^{coh}. For the scheme of Fig. 2, C^2 and C^3 (C^1) exceed(s) C^{coh} when $\bar{n} > 0.36$ ($\bar{n} > 0.44$). Note also that $C^3 \geq C^2$ because protocol 3 has lower noise than protocol 2. $C^2 \geq C^1$ due to the symmetry of protocol 2 with respect to the quadratures, which allows both signals to be decoded with equal efficiency. In fact, C^3 even exceeds C^{sq} for $\bar{n} > 11.28$, which is a similar result to the CC of controlled dense coding assisted by a measurement on the collaborator's mode [34].

In conclusion, we have demonstrated experimentally that there are fully separable and only globally nonclassical three-mode states that can lead to entanglement using a beam splitter. A similar effect happens also in the qubit case, where the CNOT gate can generate entanglement by acting on a part of a suitable three-qubit fully separable state, whereas it leaves the output of the operation separable [26]. The local state may appear unsuitable as a quantum resource. However, when being a part of a larger correlated state, it can become a source of tailored entanglement. This highlights the relevance of global correlations in quantum technologies.
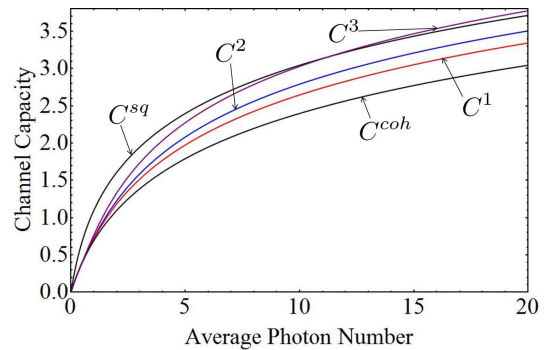
FIG. 3: Channel capacities C^1, C^2 and C^3 for the protocols 1,2 and 3 versus the average photon number. C^{sq} (C^{coh}): capacity of squeezed (coherent) state communication.

[1] A. Einstein, B. Podolsky, and N. Rosen, Phys. Rev. **47**, 777 (1935).

[2] A. Furusawa, J. L. Sørensen, S. L. Braunstein, C. A.

Fuchs, H. J. Kimble, and E. S. Polzik, Science **282**, 706 (1998).

[3] Ch. Silberhorn, P. K. Lam, O. Weiß, F. König, N. Korolkova, and G. Leuchs, Phys. Rev. Lett. **86**, 4267 (2001).

[4] X. Li, Q. Pan, J. Jing, J. Zhang, Ch. Xie, and K. Peng, Phys. Rev. Lett. **88**, 047904 (2002).

[5] T. C. Ralph, Phys. Rev. A **62**, 062306 (2000); F. Grosshans and P. Grangier, Phys. Rev. A **64**, 010301 (2001).

[6] Ch. Silberhorn, N. Korolkova, and G. Leuchs, Phys. Rev. Lett. **88**, 167902 (2002); T. Eberle, V. Händchen, J. Duhme, T. Franz, F. Furrer, R. Schnabel, and R. F. Werner, New J. Phys. **15**, 053049 (2013).

[7] W. Xiang-bin, Phys. Rev. A **66**, 024303 (2002).

[8] M. S. Kim, W. Son, V. Bužek, and P. L. Knight, Phys. Rev. A **65**, 032323 (2002).

[9] M. Brunelli, C. Benedetti, S. Olivares, A. Ferraro, and M. G. A. Paris, Phys. Rev. A **91**, 062315 (2015).

[10] S. L. Braunstein and P. van Loock, Rev. Mod. Phys. **77**, 513577 (2005); C. Weedbrook, S. Pirandola, R. García-Patrón, N. Cerf, T. Ralph, J. Shapiro, and S. Lloyd, Rev. Mod. Phys. **84**, 621669 (2012).

[11] J. Fiurášek and J. Peřina, Quantum statistics of light propagating in nonlinear optical couplers. In J. Peřina, editor, *Coherence and Statistics of Photons and Atoms*, chapter 2, pages 65-110. J. Wiley, New York, 2001.

[12] M. M. Wolf, J. Eisert, and M. B. Plenio, Phys. Rev. Lett. **90**, 047904 (2003).

[13] L. Mišta, Jr. and N. Korolkova, Phys. Rev. A **77**, 050302 (2008); L. Mišta, Jr. and N. Korolkova, Phys. Rev. A **80**, 032310 (2009).

[14] Ch. Peuntinger, V. Chille, L. Mišta, Jr., N. Korolkova, M. Förtsch, J. Korger, Ch. Marquardt, and G. Leuchs, Phys. Rev. Lett. **111**, 230506 (2013).

[15] C. E. Vollmer, D. Schulze, T. Eberle, V. Händchen, J. Fiurášek, and R. Schnabel, Phys. Rev. Lett. **111**, 230505 (2013).

[16] L. Mišta, Jr., Phys. Rev. A. **87**, 062326 (2013).

[17] R. Glauber, Phys. Rev. **131**, 2766 (1963).

[18] E. C. G. Sudarshan, Phys. Rev. Lett. **10**, 277 (1963).

[19] R. Simon, N. Mukunda, and B. Dutta, Phys. Rev. A **49**, 1567 (1994).

[20] R. F. Werner and M. M. Wolf, Phys. Rev. Lett. **86**, 3658 (2001).

[21] L.-M. Duan, G. Giedke, J. I. Cirac, and P. Zoller, Phys. Rev. Lett. **84**, 2722 (2000).

[22] R. Simon, Phys. Rev. Lett. **84**, 2726 (2000).

[23] J. Heersink, V. Josse, G. Leuchs, and U. L. Andersen, Opt. Lett. **30** (10), 1192 (2005).

[24] G. Leuchs, T. C. Ralph, Ch. Silberhorn, and N. Korolkova, J. Mod. Opt. **46**, 1927 (1999).

[25] R. Dong, J. Heersink, J.-I. Yoshikawa, O. Glöckl, U. L. Andersen, and G. Leuchs, New J. Phys. **9**, 410 (2007).

[26] T. S. Cubitt, F. Verstraete, W. Dür and J. I. Cirac, Phys. Rev. Lett. **91**, 037902 (2003).

[27] V. Chille, N. Quinn, Ch. Peuntinger, C. Croal, L. Mišta, Jr., Ch. Marquardt, G. Leuchs, and N. Korolkova, Phys. Rev. A **91**, 050301(R) (2015).

[28] V. Giovannetti, S. Mancini, D. Vitali, and P. Tombesi, Phys. Rev. A **67**, 022320 (2002).

[29] C. H. Bennett and S. J. Wiesner, Phys. Rev. Lett. **69**, 2881 (1992).

[30] S. L. Braunstein and H. J. Kimble, Phys. Rev. Lett. **61**, 042302 (2000).

[31] J. C. Hao, C. F. Li, and G. C. Guo, Phys. Rev. A **63**, 054301 (2001).

[32] C. E. Shannon, Bell Syst. Tech. J. **27**, 623 (1948).

[33] Y. Yamamoto and H. A. Haus, Rev. Mod. Phys. **58**, 1001 (1986).

[34] J. Jing, J. Zhang, Y. Yan, F. Zhao, Ch. Xie, and K. Peng, Phys. Rev. Lett. **90**, 167903 (2003).